

# Refractive index of cubic zirconia stabilized with yttria

D. L. Wood and K. Nassau

The optical transmission and indices of refraction for the cubic isomorph of  $ZrO_2$  stabilized with 12.0-mol %  $Y_2O_3$  were measured at various temperatures and for a range of wavelengths from 0.36 to 5.1  $\mu m$ . Index data to  $\pm 5 \times 10^{-5}$  were fitted to a three-term Sellmeier equation. The value of  $N_D = 2.15847$ . The dispersion  $N_G - N_B = 0.06044$ , while that for  $N_C - N_F = 0.03455$ . The temperature coefficient of the refractive index between 20 and 130°C varies from  $1.6 \times 10^{-5}/K$  for 0.36- $\mu m$  radiation to  $0.62 \times 10^{-5}/K$  for 1.6- $\mu m$  radiation.

## I. Introduction

Several crystalline forms of zirconia are known. The stable monoclinic form is found in nature as the mineral baddeleyite,<sup>1-3</sup> while at elevated temperatures there are unstable tetragonal,<sup>4</sup> hexagonal,<sup>5,6</sup> and cubic<sup>7</sup> polymorphs. The cubic form can also be stabilized at room temperature with  $MgO$ ,<sup>8</sup>  $CaO$ ,<sup>9</sup> or  $Y_2O_3$ .<sup>10</sup> It has also been observed in nature as a microcrystalline component of metamict zircon,<sup>6</sup> although the mineral has not been given a special name. Man-made stabilized cubic zirconia is being produced in the U.S.A.<sup>11,12</sup> and in Russia<sup>13</sup> with  $Y_2O_3$  stabilization and in Switzerland<sup>14</sup> with  $CaO$  stabilization. The most common product contains from 9 to 15%  $Y_2O_3$ , and we have measured the optical transmission and refractive index of a typical specimen from the U.S.A. containing 12.0-mol %  $Y_2O_3$ . Because of its large refractive index and resistance to abrasion, the material could prove useful for refractometer prisms for high-index materials.

## II. Experimental

Our sample was made by J. F. Wenckus of the Ceres Corp. by the skull-melting process<sup>11,12,15</sup> and is typical of material used in the gem trade as a diamond substitute.<sup>12</sup> A prism with faces  $\sim 11$ -mm square was cut from a single crystal with an apex angle of  $\sim 24^\circ$  and polished flat to less than one wavelength of visible ( $N_D$ ) light by conventional techniques. A plane-parallel section 0.172 cm thick was also cut from the same crystal and polished for transmission measurements. Analysis

by x-ray fluorescence and emission spectrographic methods showed no impurities above 0.01% except  $Y_2O_3$ , which was present at the level of 12.0 mol %.

The transparency of the material was measured on standard spectrophotometers covering either the UV-visible range or the infrared range. The refractive indices at seventy wavelengths between 0.36 and 5.0  $\mu m$  were measured by determining the angle of deviation for each wavelength through the prism. The apparatus has been described elsewhere.<sup>16</sup> It uses an autocollimation method, with the rear surface of the prism coated with a reflecting aluminum layer in a Littrow-type spectrometer of 25-cm focal length. The prism is rotated under computer control, with angles measured by means of a 20-bit digital shaft encoder on which the prism table is mounted. The computer program drives the prism to a series of angle settings and records the intensity of radiation passing the exit slit together with the prism temperature for each angle. The angles for maximum or minimum intensity corresponding to the standard emission or absorption lines are then converted to refractive index using Snell's law, which relates index to the angle of incidence on the prism face, and the prism apex angle. Wavelengths are selected from emission lines of spectral lamps (Hg, Cd, Cs, He, and Na), from well-known absorption lines<sup>17</sup> ( $H_2O$ ,  $CO_2$ , polystyrene), or from narrow passband optical filters.

The temperature coefficient of the refractive index is measured in a separate set of experiments by enclosing the prism in a heated jacket and measuring the rotations for various standard emission lines at elevated temperatures in the same manner as for room temperature. The slope of the index vs temperature plot gives the temperature coefficient of index.

## III. Results and Discussion

Figure 1 shows that there is essentially no absorption in cubic zirconia from 0.4  $\mu m$  at the edge of the ultraviolet to 5  $\mu m$  in the infrared. Outside that range there

The authors are with Bell Laboratories, Murray Hill, New Jersey 07974.

Received 5 March 1982.

0003-6935/82/162978-04\$01.00/0.

© 1982 Optical Society of America.

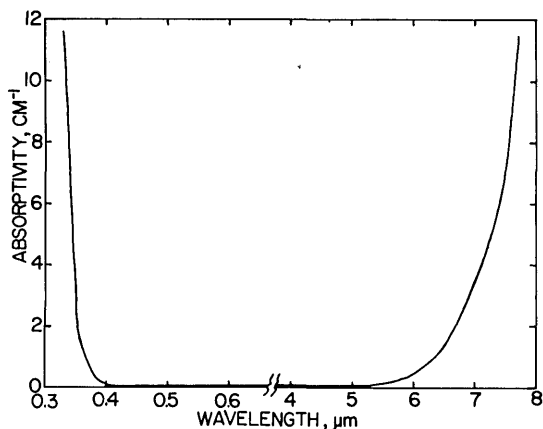


Fig. 1. Optical transmission of cubic zirconia as a function of wavelength.

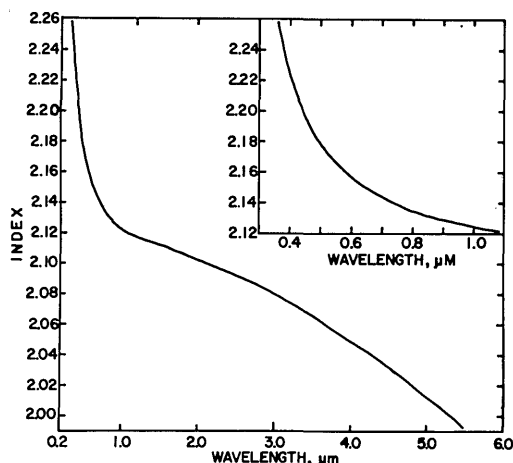


Fig. 2. Refractive index of cubic zirconia as a function of wavelength.

is strong electronic absorption in the UV and strong lattice vibrational absorption in the infrared. A correction to the apparent absorption for the 0.172-cm thick samples was made for reflection losses from the two surfaces of the plate according to the simplified relation

$$\alpha t = \log_{10} \frac{I_0}{I} - 2 \log_{10} \left| 1 - \frac{n-1}{n+1} \right|^2,$$

where  $\alpha$  is the absorptivity  $\text{cm}^{-1}$ ,  $t$  is the sample thickness in cm,  $I_0$  is the incident radiation intensity,  $I$  is the intensity of radiation passing through the sample, and  $n$  is the index of refraction at the relevant wavelengths.

The refractive-index results are presented in Table I and in Fig. 2. The wavelength, the index at 25°C, and the source of the standard wavelength are given in the first three columns of Table I. We found it convenient to measure the prism temperature during the index measurement and correct the observed index to 25°C using the temperature coefficient of index at the rele-

Table I. Indices of Refraction of Cubic Zirconia at 25°C

Source	Wavelength $\mu\text{m}$	Measured Index	Calculated Index	Difference $\times 10^5$
Cd	0.361051	2.25364	2.253572	6.8
Hg	0.365015	2.24990	2.249876	2.4
Hg	0.365483	2.24947	2.249449	2.1
Hg	0.366308	2.24871	2.248703	0.7
He	0.388865	2.23052	2.230543	-2.3
Hg	0.404656	2.21986	2.219987	-12.7
Hg	0.435833	2.20290	2.203017	-11.7
He	0.447148	2.19783	2.197864	-3.4
Cd	0.467815	2.18956	2.189540	2.0
Cd	0.479991	2.18523	2.185199	3.1
He	0.492193	2.18120	2.181209	-0.9
He	0.501567	2.17835	2.178362	-1.2
Cd	0.508582	2.17639	2.176345	4.5
Hg	0.546073	2.16694	2.166973	-3.3
Hg	0.576959	2.16066	2.160687	-2.7
Hg	0.579066	2.16026	2.160297	-3.7
He	0.587566	2.15878	2.158769	1.1
Cs	0.601033	2.15649	2.156486	0.4
Cs	0.621287	2.15334	2.153340	0.0
Cd	0.643847	2.15026	2.150193	6.7
Cs	0.658651	2.14833	2.148305	2.5
Cs	0.662865	2.14781	2.147791	1.9
He	0.667815	2.14723	2.147200	3.0
Cs	0.672328	2.14669	2.146672	1.8
Cs	0.687045	2.14503	2.145024	0.6
Cs	0.697329	2.14394	2.143934	0.6
He	0.706518	2.14303	2.143000	3.0
Cs	0.722853	2.14144	2.141424	1.6
Cs	0.727995	2.14097	2.140950	2.0
He	0.728135	2.14098	2.140937	4.3
Cs	0.760901	2.13812	2.138132	-1.2
Cs	0.794411	2.13559	2.135599	-0.9
Cs	0.852110	2.13192	2.131872	4.8
Cs	0.894350	2.12959	2.129545	4.5
Cs	0.917224	2.12842	2.128400	2.0
Cs	1.002439	2.12476	2.124692	6.8
Cs	1.012360	2.12437	2.124308	6.2
Hg	1.013975	2.12425	2.124247	0.3
Cd	1.039460	2.12338	2.123301	7.9
He	1.083030	2.12184	2.121796	4.4
Hg	1.128660	2.12038	2.120349	3.1
CHCl <sub>3</sub>	1.14800	2.11967	2.119769	-9.9
Hg	1.188900	2.11861	2.118600	1.0
Hg	1.197730	2.11817	2.118357	-18.7
Hg	1.357021	2.11439	2.114400	-1.0
Cs	1.35890	2.11435	2.114358	-0.8
Hg	1.367531	2.11421	2.114166	4.4
Hg	1.395055	2.11358	2.113547	3.3
CHCl <sub>3</sub>	1.40800	2.11319	2.113262	-7.2
Cs	1.45950	2.11194	2.111944	-0.4
Hg	1.529582	2.11072	2.110703	1.7
CHCl <sub>3</sub>	1.68800	2.10747	2.107568	-9.8
Hg	1.69272	2.10749	2.107476	1.4
Hg	1.71281	2.10716	2.107088	7.2
Filter	1.80000	2.10534	2.105415	-7.5
CHCl <sub>3</sub>	1.8600	2.10425	2.104269	-1.9
Filter	1.9650	2.10219	2.102259	-6.9
He	2.05809	2.10047	2.100461	0.9
Filter	2.2280	2.09707	2.097109	-3.9
CHCl <sub>3</sub>	2.3710	2.09419	2.094192	-0.2
Filter	2.3890	2.09381	2.093817	-0.7
Polystyrene	3.2700	2.07295	2.072886	6.4
Polystyrene	3.3000	2.07203	2.072072	-4.2
Polystyrene	3.4250	2.06869	2.068597	9.3
Polystyrene	3.5050	2.06633	2.066305	2.5
CO <sub>2</sub>	4.2250	2.04282	2.043115	-29.5
CO <sub>2</sub>	4.2710	2.04127	2.041470	-20.0
Benzene	5.0790	2.00916	2.009056	10.4
Benzene	5.1200	2.00732	2.007225	9.5
Polystyrene	5.1350	2.00664	2.006551	8.9

vant wavelength determined in the manner described earlier.

The index values at 25°C were fitted to a three-term Sellmeier equation<sup>18</sup> by a nonlinear least-squares fitting program using the relation

$$n^2 - 1 = \sum_{i=1}^3 \frac{A_i \lambda^2}{\lambda^2 - L_i^2}.$$

The constants  $A_i$  and  $L_i$  are given in Table II, and  $\lambda$  is the wavelength for which the index is  $n$ . Calculated values from this formula are also given for each wavelength in Table I, and the residuals between calculated and measured values are given in the last column of the

**Table II. Constants for Three-Term Sellmeier Equation for Refractive Indices of Cubic Zirconia at 25°C**

Constant	Value	Constant	Value
$A_1$	2.117788	$L_1$	0.166739
$A_2$	1.347091	$L_2$	0.062543
$A_3$	9.452943	$L_3$	24.320570

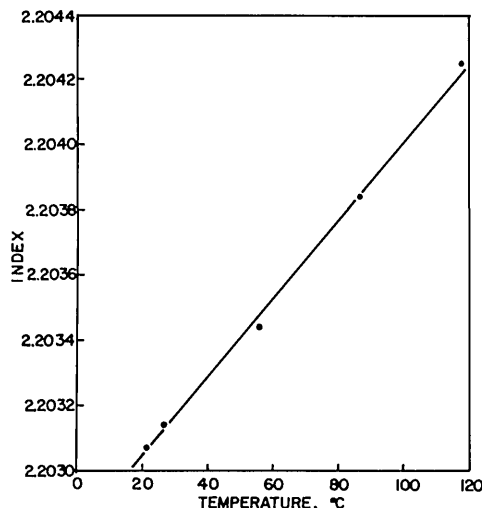


Fig. 3. Temperature dependence of refractive index for the mercury blue line  $0.435835 \mu\text{m}$  in cubic zirconia.

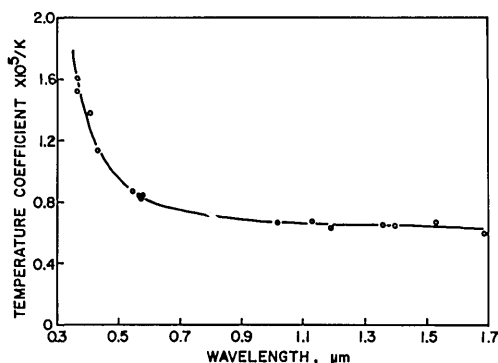


Fig. 4. Temperature coefficient of refractive index at various wavelengths for cubic zirconia.

table. The formula can be conveniently used to interpolate between the experimental values in the table. We believe that the indices are accurate to  $\pm 5 \times 10^{-5}$ .

The curves in Fig. 2 show the index of refraction decreasing rapidly with wavelength in the UV and visible regions near the absorption edge, and a slower decrease with wavelength in the infrared. The shape is typical of most transparent solids, but the value of the index of refraction is quite large,  $N_D = 2.15847$  (at  $\lambda = 0.5893 \mu\text{m}$ ); almost that of diamond,<sup>19</sup>  $N_D = 2.4175$ . The

dispersion of cubic zirconia is even larger than that of diamond,<sup>19</sup> as  $N_C - N_F = 0.03455$  for zirconia, where  $\lambda_C = 0.6563 \mu\text{m}$  and  $\lambda_F = 0.4861 \mu\text{m}$  compared to diamond, where  $N_C - N_F = 0.0250$ . The dispersion can also be expressed as  $N_B - N_G$ , where  $\lambda_B = 0.6870 \mu\text{m}$  and  $\lambda_G = 0.4308 \mu\text{m}$ , and this quantity for cubic zirconia is  $N_B - N_G = 0.06044$  compared to 0.044 for diamond.

In Fig. 3 the results for measurement of the refractive index at various temperatures between 20 and 120°C are shown for a typical mercury line  $\lambda = 0.4358 \mu\text{m}$ . The index increases linearly with temperature within the accuracy of the measurement, and the slope of the curve was  $1.14 \times 10^{-5}/\text{K}$ . This and similarly determined values for thirteen other wavelengths between 0.36 and 1.69  $\mu\text{m}$  are shown in Fig. 4, where it is clear that the temperature coefficients are relatively constant in the infrared (between  $0.62 \times 10^{-5}/\text{K}$  at 1.69  $\mu\text{m}$  and  $0.72 \times 10^{-5}/\text{K}$  at 0.8  $\mu\text{m}$ ). In contrast, a sharp increase in the coefficients is observed at shorter wavelengths in the visible and near UV.

Any change of index with temperature is mainly determined by the balance of two opposing mechanisms.<sup>20</sup> In the one mechanism tending toward a negative coefficient, increasing temperature produces a decrease in density and, therefore, a decrease in refractive index. In the other mechanism tending toward a positive coefficient, increasing temperature shifts the absorption edge (bandgap) of the material toward longer wavelength, producing an increase in refractive index. The latter mechanism is greater at shorter wavelengths closer to the absorption edge and explains the experimentally observed steeper rise in coefficient shown in Fig. 4 between 0.7 ( $0.75 \times 10^{-5}/\text{K}$ ) and 0.36  $\mu\text{m}$  ( $1.60 \times 10^{-5}/\text{K}$ ). The fact that the coefficient is never zero or negative suggests that the change of index with bulk expansion is too small to overcome the dominant bandgap shift with temperature.

#### IV. Summary

The indices of refraction for yttria stabilized cubic zirconia were measured at seventy wavelengths in the region of transparency between 0.36  $\mu\text{m}$  in the UV and 5.0  $\mu\text{m}$  in the infrared. The index data were fitted to a three-term Sellmeier equation useful for interpolation at any wavelength. Temperature coefficients of refractive index were measured for fourteen wavelengths between 0.36 and 1.69  $\mu\text{m}$ , and the measured values were used to correct all index data to 25°C even though measurements were made at variable room temperatures. The index for sodium light was  $N_D = 2.15847$ , and the dispersion was  $N_C - N_F = 0.03455$  ( $N_G - N_B = 0.06044$ ).

We acknowledge with gratitude the contribution of a crystal specimen by J. F. Wenckus, optical transmission measurements by B. E. Prescott, emission spectrographic analyses by D. L. Nash, and assistance with apparatus by J. W. Fleming, Jr., and S. S. DeBala.

## References

1. J. D. H. Donnay and H. M. Ondick, *Crystal Data* (U.S. Department of Commerce, Washington, D.C., 1973), Vol. 2, pp. M85, T107, H193, C91, C96.
2. J. Adam and M. D. Rogers, *Acta Crystallogr.* **12**, 951 (1959).
3. D. K. Smith and H. W. Nekirk, *Acta Crystallogr.* **18**, 983 (1965).
4. G. Tenfer, *Acta Crystallogr.* **15**, 1187 (1962).
5. W. P. Davey, *Phys. Rev.* **27**, 798 (1926).
6. M. V. Stackelberg and K. Chudoba, "Density and Structure of Zircon. II," *Z. Kristallogr. Mineral.* **97**, 252 (1937).
7. A. G. Boganov, I. I. Cheremisin, and V. S. Rudenko, *Dokl. Akad. Nauk. SSSR* **160**, 1065 (1965).
8. I. E. Campbell and E. M. Sherwood, Eds., *High Temperature Materials and Technology* (Wiley, New York, 1967), p. 142.
9. P. S. Duwez, F. Odell, and F. H. Brown, *J. Am. Ceram. Soc.* **35**, 107 (1952).
10. P. S. Duwez, F. H. Brown and F. Odell, *J. Electrochem. Soc.* **98**, 356 (1951).
11. J. F. Wenckus, W. P. Menashi, and R. A. Castonguay, "Cold Crucible System," U.S. Patent 4,049,384, 20 Sept. 1977.
12. K. Nassau, *Lapidary J.* **31**, 900, 922 (1977); **35**, 1194 (1981).
13. Z. I. Alexandrov, V. V. Osiko, V. M. Tatarintsev, and V. T. Udovenchik, "Monocrystals Based on Stabilized Zirconium or Hafnium Dioxide and Method of Production Thereof," U.S. Patent 4,153,469, 8 May 1979.
14. E. Gubelin, "Djevalith-eine neue Diamant-Imitation" *Z. Dtsch. Gemmol. Ges.* **25**(4), 204-210 (1976).
15. J. F. Wenckus, M. L. Cohen, A. G. Emslie, W. P. Menashi, and P. F. Strong, "Study, Design and Fabrication of a Cold Crucible System," Air Force Cambridge Research Laboratory Final report AFCRL-TR-75-0213, 31 Mar. 1975.
16. D. L. Wood and J. W. Fleming, Jr. *Rev. Sci. Instrum.* **53**, 43 (1982).
17. H. W. Thompson, Ed. *IUPAC Tables of Wavenumbers for the Calibration of Infrared Spectrometers* (Butterworths, Washington, 1961).
18. L. E. Sutton and O. N. Stavroudis, *J. Opt. Soc. Am.* **51**, 901 (1961).
19. S. Rosch, *Opt. Acta* **12**, 253 (1965); W. G. Driscoll, Ed, *Handbook of Optics* (McGraw-Hill, New York, 1978), pp. 7-82.
20. Y. Tsay, B. Bendow, and S. S. Mitra, *Phys. Rev.* **138**, 2688 (1973).

Books continued from page 2964

scattering as well as the most introductory part of the theory of light scattering. Cardona's intent in writing this chapter appears to be to present in one place a coherent and unified picture of resonant light scattering phenomena. I found this chapter particularly useful to experimentalists who are constantly searching for consistent notations, normalization conventions, and other details to make close contacts between measured data and various theoretical parameters. The section on absolute scattering cross sections presents a good summary of existing data and measuring methods. One can clearly sense that this chapter was written by a seasoned experimentalist who is well versed in both theory and experimental details. One criticism that I have is that it contains some topics that are not necessarily close to the chapter's main theme. Or perhaps I was misled by the title. A student trying to learn about resonant light scattering phenomena may become unnecessarily confused and derailed from the main track of the reasoning by inclusion of such subjects as light scattering in amorphous and disordered materials and defect-induced Raman spectra. On the other hand, if you know what you are looking for, you will find this chapter a most up-to-date and useful review.

Since many researchers are considering adoption of optical multi-channel analyzer (OMA) systems to replace photomultipliers, Chap. 3 comes as a timely and useful review of this newly available detection method in optical spectroscopy. This chapter describes the principles of OMA operation as well as the required characteristics of a spectrometer to be used with OMA and several unique uses for OMAs.

The last chapter presents a concise review of several four-wave mixing phenomena related to Raman scattering. The basic principles involved in such nonlinear spectroscopic techniques as CARS, RIKES, and HRS are outlined in a unified way, and several experimental applications of these phenomena in solids are presented. This is a useful chapter for the reader new to the field who is trying to sort out the relationship among many techniques designated by acronyms.

Light scattering is still a rapidly expanding field in which current information is only in a fragmented form in journals. Therefore, this book serves a useful purpose by making the latest information available in a systematic and ordered fashion. We can all look forward to publication of future volumes of this series.

S. USHIODA

**Catastrophe Theory for Scientists and Engineers.** By ROBERT GILMORE. John Wiley & Sons, New York, 1981. 665 pp. \$45.95.

The book is divided into four parts containing a total of twenty-three chapters; an epilogue and author and subject indices complete the volume. A first glimpse in the book convinces anyone that it is a special contribution to the bibliography of catastrophe theory.

The content of the first two parts may be considered independent from the rest of the book in that these parts may constitute an integral form of a book relating to elementary catastrophe theory and its applications. This fact does not mean that the last two parts are not useful. On the contrary, the organization of the book makes it useful not only to those who are interested in learning what is elementary catastrophe theory and where it can be applied, but also to those inquisitive ones who want to learn further details of catastrophe theory itself.

In fact, the first part of the book contains the mathematics of elementary catastrophe theory at an elementary level thus proving that elementary catastrophe theory is an extension of elementary differential calculus, a knowledge of which is the only prerequisite for understanding this part. If one considers the jargon used in all previous literature on catastrophe theory which is based on differential topology, he will understand the contribution of the author to a large audience of applied scientists who are not familiar with this branch of mathematics.

The fourth part could take the place of the second, since it contains the mathematics of elementary catastrophe theory in somewhat more detail by stating Thom's theorem (without proof) as well as some new mathematical terminology necessary for a thorough study by the demanding reader.

The second part contains applications of elementary catastrophe theory to several fields of science, which are presented in an explicit and clear way. Finally the purpose of the third part is to show the possibilities of extending elementary catastrophe theory and its seven elementary catastrophes, as they have been described by Thom, to more complicated functions—a very interesting subject to mathematical physicists.

The contents of the book may be described in some detail as follows:

continued on page 2991